



Growth characteristics and electrical properties of Ta₂O₅ grown by thermal and O₃-based atomic layer deposition on TiN substrates for metal–insulator–metal capacitor applications

Min-Kyu Kim^a, Woo-Hee Kim^b, Taeyoon Lee^a, Hyungjun Kim^{a,*}

^a School of Electrical and Electronic Engineering, Yonsei University, 262 Seongsanno, Seodaemun-gu, Seoul 120-749, Republic of Korea

^b Process Development Team, System LSI Division, Samsung Electronics, San #24 Nongseo-Dong, Giheung-Gu, Yongin-City, Gyeonggi-Do 446-711, Republic of Korea

ARTICLE INFO

Article history:

Received 8 October 2012

Received in revised form 12 June 2013

Accepted 12 June 2013

Available online 5 July 2013

Keywords:

Atomic layer deposition

Tantalum pentoxide

Ozone-based atomic layer deposition

Metal–insulator–metal capacitor

ABSTRACT

We compared the suitability of tantalum pentoxide (Ta₂O₅) films produced via thermal and ozone based atomic layer deposition (Th-ALD and O₃-ALD, respectively) using pentaethoxytantalum (PET) as a Ta precursor for use as a capacitor insulator in metal–insulator–metal configurations. H₂O and O₃ were used as reactants for Th-ALD and O₃-ALD Ta₂O₅, respectively. Both of the processes exhibited ALD mode growth with good self-saturation behavior and produced pure Ta₂O₅ films. However, O₃-ALD Ta₂O₅ films showed higher growth rates (1.1 Å/cycle), density (7.85 g/cm³) and dielectric constant values (~46) compared to those of Th-ALD Ta₂O₅ (0.9 Å/cycle, 7.3 g/cm³ and ~40, respectively).

© 2013 Elsevier B.V. All rights reserved.

1. Introduction

Among high-*k* gate oxide materials, tantalum pentoxide (Ta₂O₅) is one of the most promising due to its high dielectric constant (22–60), low leakage current, good dielectric breakdown strength, thermal and chemical stability, and other qualities [1–8]. Due to its technical importance, a number of thin film deposition techniques have been employed to deposit Ta₂O₅, including chemical vapor deposition and physical vapor deposition [5–14]. Atomic layer deposition (ALD), however, has received a great deal of attention as a promising method for the deposition of capacitor electrodes in nanoscale dynamic random access memory devices due to its excellent conformality and atomic scale controllability [15–17].

Precursors such as Ta(OC₂H₅)₅, Ta(OCH₃)₅, Ta(thd)₄Cl, and TaCl₅ have been studied for ALD and CVD of Ta₂O₅ [5–14]. While metal halides including TaCl₅ have been widely employed as ALD precursors due to their excellent thermal stability, there is an increasing need for halogen-free metalorganic ALD precursors to avoid the formation of corrosive hydrogen halide byproducts during growth and of halide impurities in films. Additionally, Ta₂O₅ ALD growth rates from TaCl₅ and water decrease at 280 °C due to etching of the deposited film [16]. Ta₂O₅ films deposited using most available tantalum alkoxide precursors have relatively high levels of carbon impurities when compared to films grown using precursors with chloride ligands [18,19].

According to previous studies, Ta₂O₅ films with very low carbon contents may be grown from Ta(OC₂H₅)₅ by CVD and ALD methods [13,19].

The most widely studied oxidant for ALD is water (H₂O) [5–11,19]. However, since H₂O tends to physisorb strongly onto surfaces, the purge time needed to sufficiently remove the physisorbed H₂O from the reactor surface may be long, especially at low temperatures [20]. In previous reports, we showed that plasma-enhanced atomic layer deposited (PE-ALD) oxides have superior properties such as high film density, high growth rate, low equivalent oxide thickness and low leakage currents, compared to Th-ALD (thermal ALD) [21,22]. In addition, a previous report on plasma-enhanced CVD Ta₂O₅ revealed extremely low levels of leakage currents for MOS capacitors [23]. Despite these advantages, PE-ALD has not been commercialized due to difficulties associated with its mass production and poor conformality [24]. Ozone (O₃) is a strong oxidizing agent and is highly volatile, which makes it one of the most promising alternative oxygen sources for use in ALD processes. In addition, the electrical performance of Ta₂O₅ film is critically dependent on post-deposition annealing in oxygen or ozone, which is required to lower oxygen deficiencies and carbon impurities in the film. Therefore, we hypothesized that O₃-ALD Ta₂O₅ could benefit from same process. The production of O₃-based ALD Ta₂O₅ using Ta(OC₂H₅)₅ has been reported only rarely, and no reports comparing thermal ALDs (H₂O-based ALD) have been published.

Meanwhile, TiN is one of the most widely used materials for top and bottom electrodes in metal/insulator/metal (MIM) capacitors, as well as barrier and gate electrodes, since it has a low leakage current and good voltage linearity due to its good chemical stability and high barrier height when used with most dielectrics (~2 eV with Ta₂O₅

* Corresponding author. Tel.: +82 2 2123 5773.

E-mail address: hyungjun@yonsei.ac.kr (H. Kim).

dielectric). In addition, its etching process is well-established compared to those of noble metals including Ru and Pt [25]. However, TiN thin films have strong oxidation tendencies. Although typical ALD processing temperatures for high k oxide are relatively low [26], the presence of highly reactive ozone is expected to enhance oxidation rates and could result in detrimental effects on device performance such as high leakage currents caused by TiO_x formation between the dielectric layer and TiN [27].

In this study, we investigated the growth characteristics and film properties of thermal ALD and O_3 -based ALD Ta_2O_5 using $\text{Ta}(\text{OC}_2\text{H}_5)_5$ as a Ta precursor and H_2O and O_3 as reactants. The growth characteristics were studied as functions of key growth parameters including reactant exposure time, growth cycles, and substrate temperature. Then, the film properties and electrical properties were compared using several film analysis techniques. O_3 -based ALD Ta_2O_5 showed superior electrical properties to thermal ALD Ta_2O_5 for use as an insulator in MIM capacitors, such as a higher dielectric constant and lower leakage currents.

2. Experimental details

A commercial ALD chamber (SNTEK Co., ALD5008) equipped with an ozone generator (ASTeX Inc., AX8406A) was used for this study. This configuration has a double shower head system to achieve good uniformity with plasma capability. Pentaethoxytantalum (PET, $\text{Ta}(\text{OC}_2\text{H}_5)_5$) was employed as a Ta precursor. The bubbler temperature for mixtures containing PET was maintained at 160 °C to produce sufficiently high vapor pressure [13,28], while the delivery lines were heated to temperatures 10–15 °C higher than the bubbler to avoid precursor condensation. To improve gas delivery, vaporized precursor molecules were carried to the reaction chamber using Ar gas, at flow rates that were controlled using a mass flow controller. For Th-ALD, a bubbler containing water was immersed in silicone oil for temperature control and water vapor flow was controlled using a leak valve. For O_3 -ALD, oxygen gas and nitrogen were flowed into an ozone generator that was set to generate ozone at rates higher than 250 g/m^3 .

Impurity levels, chemical composition, and binding structures were analyzed by X-ray photoelectron spectroscopy (XPS, Escalab 220i-XL) with a monochromatic Al $K\alpha$ source (beam energy: 1486.6 eV, analysis energy step: 0.1 eV and analysis area: 100 μm^2), where surface C 1s peak at 284.5 eV was used as a reference to calibrate the measured core levels. Film thickness, density, and roughness were measured by X-ray reflectivity (XRR) with Cu $K\alpha$ radiation (PANalytical X'Pert PRO). Information on stacking order and multilayer materials, including the substrate (TiN 25 nm/ SiO_2 100 nm), is useful to reduce degrees of freedom in XRR analysis and simulation. Theta-2theta (θ -2 θ) X-ray diffraction (XRD) measurement with Cu $K\alpha$ radiation (Rigaku, DMAX 2400) was carried out in order to compare microstructures and crystallization of thermal ALD and O_3 -based ALD Ta_2O_5 films. The electrical properties of the MIM capacitors were evaluated using capacitance–voltage (C–V) and current–voltage (I–V) measurements.

Ta_2O_5 MIM capacitors were fabricated on CVD TiN/ SiO_2 substrates. For MIM capacitor fabrication, Ru was deposited as a top electrode through a patterned shadow mask by magnetron sputtering. To reduce trap charge densities, post deposition annealing and forming gas annealing were carried out at 400 °C for 10 min in a nitrogen environment, and for 30 min in H_2 5%– N_2 95%, respectively. Electrical properties including C–V and I–V characteristics were measured using a Keithley 590 CV analyzer with a Keithley 236 source analyzer unit.

3. Results and discussion

Fig. 1a shows the dependence of film growth rates (thickness per cycle) of Th-ALD and O_3 -ALD Ta_2O_5 films as functions of reactant exposure time (t_r) at a growth temperature (T_s) of 300 °C. In both

cases, saturation in growth rate, which is a typical ALD characteristic, occurs at $t_r \geq 1$ s. The saturated growth rate of Th-ALD under saturation conditions is about 0.9 Å/cycle, which is lower than that of O_3 -ALD (1.1 Å/cycle). ALD ZrO_2 , TiO_2 , Al_2O_3 and HfO_2 exhibited higher growth rates in previous studies for O_3 -ALD than for Th-ALD, agreeing with the results of the present study [29–32]. The increased growth rates due to the use of O_3 -ALD are believed to be due to higher reactivity of oxygen radicals. O_3 dissociation into reactive O radicals occurs at 300 °C, and therefore the elimination of ligands from the surface by O radicals is expected to be more efficient than when H_2O is used [33].

Based on the saturation curve, we fixed the precursor exposure time at $t_r = 2$ s for subsequent experiments. Fig. 1b shows the dependence of film growth rates per cycle with increases in growth temperature from $T_s = 100$ to 400 °C under saturated conditions ($t_s = 2$ s and $t_r = 2$ s) for Th-ALD and O_3 -ALD Ta_2O_5 . In both cases, three regions are identified (Fig. 1b). In the middle temperature region, from $T_s = 200$ to 300 °C for Th-ALD and O_3 -ALD, the growth rates are almost constant, indicating the presence of a so-called “process window.” Meanwhile, the growth rate increases with increased growth temperature in the high and low growth temperature regions. When $T_s = 400$ °C for both methods, the growth rates were slightly increased and expected to exhibit effects associated with thermal precursor decomposition. These characteristics are observed in previous reports, including ours, regarding ALD of oxides [15–17,29–32].

Fig. 2a, b and c are XPS spectra of Th-ALD and O_3 -ALD Ta_2O_5 , showing that the locations of O 1s (529.4 eV) and two Ta 4f (location

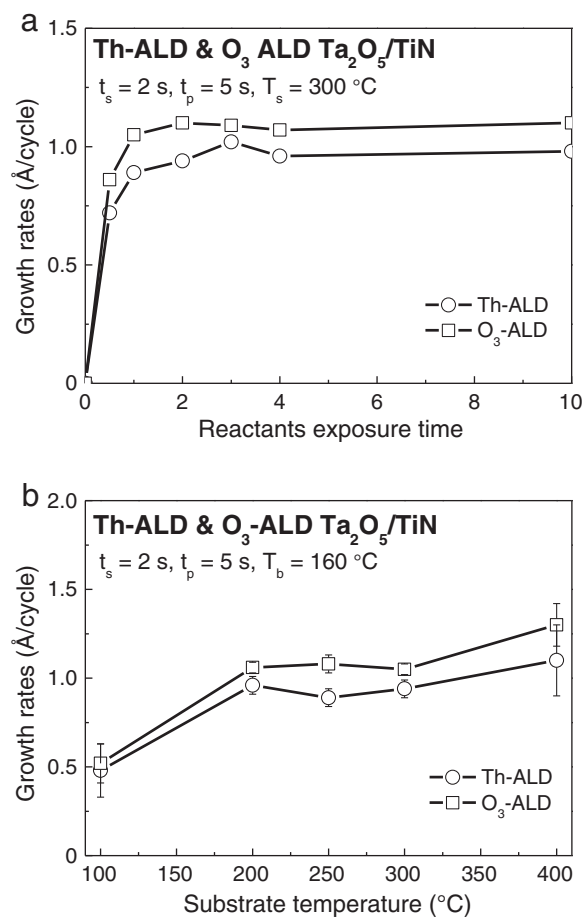


Fig. 1. Growth rates of Th-ALD and O_3 -ALD Ta_2O_5 (a) as functions of H_2O or O_3 exposure time (t_r) on TiN substrates at $T_s = 300$ °C, and (b) as a function of growth temperature T_s .

of low energy peak: 26.7 eV, interval between two peaks: 1.7 eV) peaks are similar to those observed in previous reports regarding thermal ALD and CVD Ta₂O₅ films [18,19]. After surface cleaning by sputtering with Ar + ion bombardment at an energy of 3 keV and beam current density of 22.2 μA/cm² (2 mA induced beam current, rastered over a 3 × 3 mm² area), the C concentration was lower than 1 at.% for O₃-ALD Ta₂O₅, which is also lower than most results reported for ALD using other precursors [4–8,18]. Similarly, low C concentrations were observed for Th-ALD Ta₂O₅, which were slightly higher than those of O₃-ALD Ta₂O₅. Moreover, although another group previously reported that ALD Ta₂O₅ films incorporate low C concentrations using PET [19], the O₃-ALD process with a PET precursor used in the present study has additional advantages such as higher growth rates and better process compatibility due to the liquid state of the precursor.

Meanwhile, the peak intensities of Ta 4f and O 1s for O₃-ALD were about 10% higher and sharper than that of Th-ALD. The peak intensity,

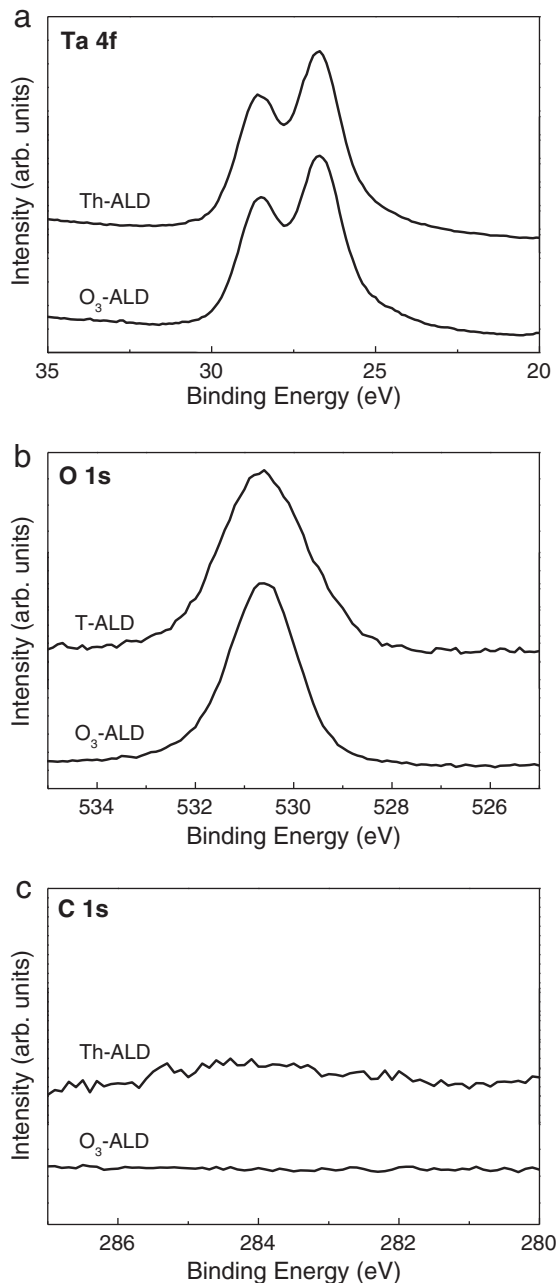


Fig. 2. (a) Ta 4f (b) O 1s and (c) C 1s XPS spectra of Th-ALD and O₃-ALD Ta₂O₅ films.

$I_{\text{Ta}_2\text{O}_5}$, is a function of density $n_{\text{Ta}_2\text{O}_5}$, photoionization cross section $\sigma_{\text{Ta}_2\text{O}_5}$, and escape depth $\lambda_{\text{Ta}_2\text{O}_5}$ [34].

$$I_{\text{La}_2\text{O}_3} = n_{\text{La}_2\text{O}_3} \sigma_{\text{La}_2\text{O}_3} \lambda_{\text{La}_2\text{O}_3} \quad (1)$$

Since photoionization cross section and escape depth (which are determined by the material itself) should be almost the same for both Th-ALD and O₃-ALD, the higher peak intensity of O₃-ALD indicates that the film density of O₃-ALD Ta₂O₅ is also higher than that of Th-ALD. In addition, the sharper shape of O₃-ALD Ta₂O₅ films indicates lower levels of Ta–OH and Ta–O–Ti bonding [35,36].

For more exact determinations of film density and other related properties, XRR analysis was performed for nominally 15 nm thick Th- and O₃ based Ta₂O₅. The resulting spectra are shown in Fig. 3 using simulated results. During simulations, we obtained the best-fit results for density, thickness and roughness using a three-layer model composed of Ta₂O₅, TiN (20 nm) and SiO₂ (100 nm) (Table 1). The film thicknesses obtained through simulations of XRR spectra were consistent with separately-measured ellipsometry data for both films. The film density (7.85 g/cm³) of O₃-ALD was much higher than that of Th-ALD (7.3 g/cm³), agreeing well with the XPS spectra. The density values of the XRR spectrum for Th-ALD agree with those previously reported for ALD Ta₂O₅ using the same PET precursor and H₂O [19]. However, there were no significant differences in surface roughness of both films.

Fig. 4a shows C–V curves for Ru/20 nm ALD Ta₂O₅/TiN MIM capacitors that were fabricated using Th-ALD and O₃-ALD. The EOT of O₃-ALD Ta₂O₅ (1.7 nm) is lower than that of Th-ALD Ta₂O₅ (2.0 nm). This observation could be explained by Clausius–Mossotti's equation, which explains the relationship between dielectric constant and film density [37]. The C–V characteristics of ALD Ta₂O₅ based on PET are superior to those of Ta₂O₅ films based on other precursors. For example, the C–V curve of CVD Ta₂O₅ films from Ta(OCH₃)₅ at 250 °C showed a lower dielectric constant (~24) [12] than the films fabricated in the present study (Th-ALD ~ 40, O₃-ALD ~ 46). The crystallinities of Ta₂O₅ films (Fig. 5) also support our results. Fig. 5 shows out-of-plane θ –2 θ XRD patterns of Ta₂O₅ films annealed at 400 °C in a nitrogen environment by an RTA system. Both of the films exhibited hexagonal δ -Ta₂O₅ structure, which is known to have high dielectric constant values up to 40 [38–40]. This finding agrees with previous reports of Ta₂O₅ fabricated using the same precursor [19]. In addition, O₃-ALD Ta₂O₅ film shows a higher intensity peak of narrow width, which is in good agreement with the density and leakage data reported below.

Fig. 4b shows leakage current densities according to electric fields for both samples. The leakage current density of the O₃-ALD sample (1.9×10^{-6} A/cm²) at –1 V is slightly lower than that of the Th-ALD sample (2.7×10^{-6} A/cm²). Similarly, other groups previously reported that the leakage current densities of MOS capacitors

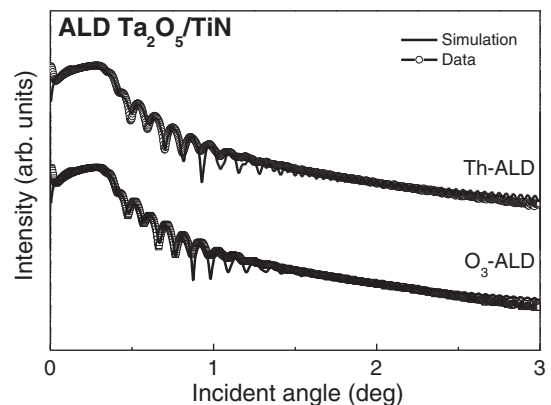


Fig. 3. XRR (open circle) and simulation fitting (solid line) data obtained from Th-ALD and O₃-ALD Ta₂O₅ films.

Table 1

X-ray reflection and ellipsometry of Th-ALD and O₃-ALD Ta₂O₅ films on CVD TiN/SiO₂/Si substrates (roughness of CVD TiN layer: 1.1 nm). The ALD process conditions were the same for both types of films ($t_s = 2$ s, $t_p = 5$ s, $t_r = 2$ s, and $T_s = 300$ °C).

	Deposition # of ALD cycles	Ellipsometer		X-ray reflection	
		Thickness	Thickness	Density	Roughness
Th-ALD	150	14.6 nm	14.3 nm	7.30 g/cm ³	1.3 nm
O ₃ -ALD	145	15.7 nm	16.4 nm	7.85 g/cm ³	1.3 nm

composed of gate oxide films prepared by O₃-ALD were lower than those prepared by Th-ALD [31,32]. However, it has only rarely been reported that the O₃-based ALD process produces improved leakage properties for MIM capacitors, as shown in this study. In addition, compared to the data reported in [11,19], which includes leakage properties for MIM capacitors fabricated using ALD Ta₂O₅, we were able to achieve superior properties even though the properties were not suitable to adapt device applications. Thus, the potential problems associated with unwanted oxidation of the bottom TiN electrode during O₃-based ALD appear to be minimal. However, the slight shift of the O₃-ALD leakage current curve that we observed could be explained by the dipole effect of Ta–O–Ti bonding caused by oxidation of the TiN bottom electrode and differences in electronegativity between Ta and Ti. The O₃-based ALD process produces capacitor insulators with improved electrical properties, including low EOT with slightly change of leakage current. These improvements are attributed to superior physical properties, such as higher film density, than conventional Th-ALD using water as a reactant.

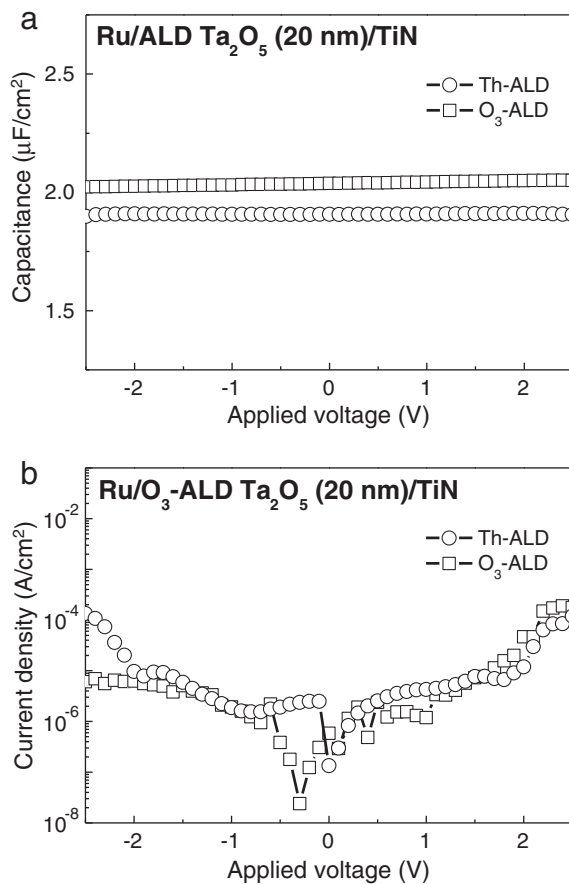


Fig. 4. (a) Capacitance–voltage curves and (b) gate leakage currents of MIM capacitors with Th-ALD and O₃-ALD Ta₂O₅ as insulators.

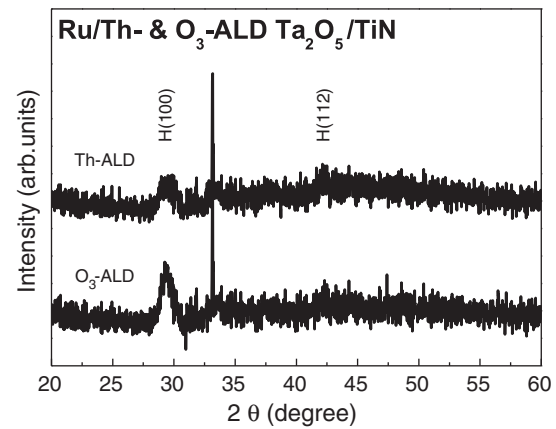


Fig. 5. XRD patterns of Th-ALD and O₃-ALD Ta₂O₅ films annealed at 400 °C in nitrogen environments using the RTA system.

4. Conclusions

For this study, we compared the results of Th-ALD and O₃-ALD Ta₂O₅ processes, including film properties. ALD growth modes were achieved for both processes, indicating good saturated growth behavior and ALD process windows. Although both Th-ALD and O₃-ALD processes produced pure Ta₂O₅ films with low C contamination, the O₃-ALD Ta₂O₅ process resulted in higher growth rates, better film quality, and better electrical properties than did Th-ALD, with no major adverse effects caused by TiN electrode oxidation. Thus, O₃-ALD Ta₂O₅ films fabricated using PET have great benefits for microelectronic engineering applications.

Acknowledgments

This work was supported by the Technology Innovation Program funded by the Future-Based Technology Development Program (Nano Fields) through the National Research Foundation of Korea (NRF), which is funded by the Ministry of Education, Science and Technology (No. 2012-0006217) and the Converging Research Center Program through the Ministry of Education, Science and Technology (2012K001311). This work was also supported by a National Research Foundation of Korea (NRF) grant funded by the Korean government (MEST) (No. 2011-0028594). Additionally, this work was supported by the Industrial Strategic Technology Development Program (10041926, Development of high density plasma technologies for thin film deposition of nanoscale semiconductor and flexible display processing) funded by the Ministry of Knowledge Economy (MKE), Korea.

References

- [1] Q. Lu, Donggun Park, Alexander Kalnitsky, Celene Chang, Chia-Cheng Cheng, Sing Pin Tay, Tsu-Jae King, Chenming Hu, IEEE Electron. Device Lett. 19 (1998) 341.
- [2] O. Engstrom, B. Raeli, S. Hall, O. Bui, M.C. Lemme, H.D.B. Gottlob, P.K. Hurley, K. Cherkaoui, Solid State Electron. 51 (4) (2007) 622.
- [3] M. Saitoh, T. Mori, H. Tamura, IEDM Tech. Dig. (1986) 680.
- [4] S.C. Sun, T.F. Chen, IEEE Electron. Device Lett. 17 (1996) 355.
- [5] M.L. Terranova, V. Guglielmotti, S. Orlanducci, V. Sessa, E. Tamburri, M. Rossi, ECS Trans. 25 (8) (2009) 1153.
- [6] E. Atanassova, T. Dimitrova, in: H.S. Nalva (Ed.), Handbook of Surfaces and Interfaces of Materials, vol. 4, Academic Press, San Diego, USA, 2001, p. 439.
- [7] C. Chaneliere, J.L. Autran, R.A.B. Devine, J. Appl. Phys. 86 (1999) 480.
- [8] E. Atanassova, D. Spassov, A. Paskaleva, Microelectron. Eng. 83 (2006) 1918.
- [9] K.M.A. Salam, H. Fukuda, S. Nomura, J. Appl. Phys. 93 (2003) 1169.
- [10] K. Kukli, M. Ritala, R. Matero, M. Leskela, J. Cryst. Growth 212 (2000) 459.
- [11] T. Blanquart, V. Longo, J. Niinisto, M. Heikkila, K. Kukli, M. Ritala, M. Leskela, Semicond. Sci. Technol. 27 (2012) 074003.
- [12] K. Yamagishi, Y. Tarui, Jpn. J. Appl. Phys. 25 (1986) 306.
- [13] P.A. Murawala, M. Sawai, T. Tatsuta, O. Tsuji, S. Fu-jita, S. Fujita, Jpn. J. Appl. Phys. 32 (1993) 368.
- [14] C.H. An, K. Sugimoto, J. Electrochem. Soc. 139 (1992) 1956.

- [15] T. Suntola, Mater. Sci. Rep. 4 (1989) 261.
- [16] H. Kim, J. Vac. Sci. Technol. B 21 (2003) 2231.
- [17] H. Kim, Han-Bo-Ram Lee, W.-J. Maeng, Thin Solid Films 517 (2009) 2563.
- [18] M. Matsui, S. Oka, K. Yamagishi, K. Kuroiwa, Y. Tarui, Jpn. J. Appl. Phys. 27 (1988) 506.
- [19] K. Kukli, M. Ritala, M. Leskela, J. Electrochem. Soc. 142 (1995) 1670.
- [20] D.M. Hausmann, E. Kim, J. Becker, R.G. Gordon, Chem. Mater. 14 (2002) 4350.
- [21] W.J. Maeng, H. Kim, Electrochem. Solid-State Lett. 9 (2006) G191.
- [22] W.H. Kim, W.J. Maeng, K.J. Moon, J.M. Myoung, H. Kim, Thin Solid Films 519 (2010) 362.
- [23] M. Seman, J.J. Robbins, S. Agarwal, C.A. Wolden, Appl. Phys. Lett. 90 (2007) 131504.
- [24] H. Kim, Thin Solid Films 519 (2011) 6639.
- [25] P. Caubet, T. Blomberg, R. Benaboud, C. Wyon, E. Blanquet, J.-P. Gonchond, M. Juhel, P. Bouvet, M. Gros-Jean, J. Michailos, C. Richard, B. Iteprat, J. Electrochem. Soc. 155 (2008) H625.
- [26] M. Wittmer, J. Noser, H. Melchior, J. Appl. Phys. 52 (11) (1981) 6659.
- [27] A.R. Bally, P. Hones, R. Sanjines, P.E. Schmid, F. Levy, Surf. Coat. Technol. 108–109 (1998) 166.
- [28] S. Kamiyama, H. Suzuki, H. Watanabe, A. Sakai, H. Kimura, J. Mizuki, J. Electrochem. Soc. 141 (1994) 1246.
- [29] K. Knapas, M. Ritala, Chem. Mater. 20 (2008) 5698.
- [30] H.J. Lee, M.H. Park, Yo-Sep Min, Guylhaine Clavel, Nicola Pinna, Cheol Seong Hwang, J. Phys. Chem. C 114 (2010) 12736.
- [31] J.B. Kim, D.R. Kwon, K. Chakrabarti, C. Lee, K.-Y. Oh, J.H. Lee, J. Appl. Phys. 92 (2002) 6739.
- [32] H.B. Park, M. Cho, J. Park, S.W. Lee, C.S. Hwang, J. Appl. Phys. 94 (2003) 3641.
- [33] O.R. Wulf, The Thermal Decomposition of Ozone., Ph.D. Thesis California Institute of Technology, Pasadena, CA, 1926.
- [34] F.J. Himpsel, F.R. McFeely, A. Taleb-Ibrahimi, J.A. Yarmoff, G. Hollinger, Phys. Rev. B 38 (9) (1988) 6084.
- [35] J.F. Moulder, W.F. Stickle, P.E. Sobol, K.D. Bomben, Handbook of X-ray Photoelectron Spectroscopy, Perkin-Elmer, Eden Prairie, MN, 1992.
- [36] Y. Takasu, M. Suzuki, H. Yang, T. Ohashi, W. Sugimoto, Electrochim. Acta 55 (2010) 8220.
- [37] P.V. Rysselberghe, J. Phys. Chem. 36 (4) (1932) 1152.
- [38] C. Chaneliere, S. Four, J.L. Autran, R.A.B. Devine, N.P. Sandler, J. Appl. Phys. 83 (1998) 4823.
- [39] Y. Nakagawa, T. Okada, J. Appl. Phys. 68 (1990) 556.
- [40] N. Rausch, E.P. Bulte, Microelectron. J. 25 (1994) 533.